RSC Advances

ROYAL SOCIETY OF CHEMISTRY

www.rsc.org/advances

Synthesis and characterization of polyurethane ionene/zinc chloride complex with antibacterial property

Bu-Peng Ding[1], *Fang Wu*[1], *Si-Chong Chen*[1], *Yu-Zhong Wang*[1*], *Jian-Bing Zeng*[2*]

Abstract

1,6-bis(*N',N*-dimethyl-3-hydroxylpropyl) ammonium chloride (BQAC-diol)/zinc chloride complex was first synthesized and used as ionic monomer to synthesize polyurethane ionene/zinc chloride (PUI/$ZnCl_2$) complex via its polymerization with poly(ethylene glycol) (PEG), 1,4-butanediol (BDO), and 4,4'-diphenylmethane diisocyanate (MDI). The structure and properties of PUI/$ZnCl_2$ complex were characterized systematically by NMR, intrinsic viscosity, thermogravimetric analysis (TGA), differential scanning calorimetry (DSC), polarized optical microscopy (POM), and tensile test, and the antibacterial property was investigated by cylinder-plate method. The results indicated that the crystallization rate of PUI/$ZnCl_2$ increased gradually with increasing content of ionic unit, which was ascribed to the increased crystal growth rate as evidenced by POM observation. The morphology analyzed by scanning electron microscopy indicated that no apparent microphase separation occurred for the complex and $ZnCl_2$ dispersed at molecular level in PUI matrix, since no particle-like specie can be observed. Antibacterial property measurement showed that the PUI containing quaternary ammonium salt cation has no antibacterial activity but the coexistence of $ZnCl_2$ and cation exhibit synergetic effect with respect to the antibacterial activity.

1. Introduction

Polymeric materials have been the most common and available products in our daily life for a long time, due to its colorful exterior, good processibility, and low cost. However, these widely used plastics can be a big threat to the health of human being, because most polymeric productions can be easily contaminated or infected by microorganisms on the surface in a variety of areas, especially in hospitals, hotels, household appliances,[1-3] and most of them do not have inherent antibacterial (AB) properties.[4] Thus there has been an explosion of demand for safe, healthy products capable of AB property against common bacteria and fungus. Currently a number of AB agents have been studied and introduced into polymer productions, including inorganic substances like silver ion,[5-7] nanoparticles,[8,9] and organic ones like common antibiotics[10,11] and quaternary ammonium salts.[12,13]

Polyurethane (PU) covers a large range of materials with various physical and thermal properties and it can be designed easily according to people's demands by tailoring or cooperating different segments.[14,15] However, PU is susceptible to be degraded by many types of bacteria during the age of service and storage.[16] Thus, it is interesting and meaningful to study the AB property of PU, and many research work has been reported on this topic. Silver ion or nano silver has long been considered to be highly biocompatible and has strong AB effects against a broad spectrum of bacteria among all the additives.[4] Although the PU and Ag system is likely to have great AB property, it is very difficult to prevent the agglomeration of nano Ag during process and usage. ZnO nanoparticle can also be filled in the polyurethane to form composite with AB property.[17] The AB property was enhanced with the increase of ZnO content, but the mechanical property and thermal stability diminished compared with the neat

material. AB function can also be provided by chemical modification of materials backbone with appropriate AB functional groups,[18,19] which attracted more interest than the AB additives mentioned above, because of non-volatility, good environmental and chemical stability.[20] One of most classical and effective AB agents should be quaternary ammonium salts (QAS), mainly due to the fact that it is a broad-spectrum bactericide and can be easily tailed for desired functionality through traditional chemical synthesis.[21-23] To introduce the QAS into polymers, a common way is to synthesize cationic monomers with quaternary ammonium groups on the pendant side, and then polymerize them.[24] QAS group can also be gained by quaternization of amine after polymerization. For example, Zhu et al[25] have reported segmented PU ionomers with shape memory function, QAS was obtained after post-quaternarization, and the AB activity against gram-positive bacteria was significant.

However, the researches on the PU containing ionic groups in the main chains remained much less active than those with pendant ionic groups attached to the polymer backbone. Ionenes, which can be synthesized by Menschutkin reaction,[26] usually show good AB properties.[27] Zinc chloride ($ZnCl_2$), as a cheap inorganic AB agent with good AB activity[28-30] can be used to enhance antibacterial properties of polymer matrix.[31] The main advantage of inorganic AB agents is stability and long shelf life, compared with the organic tantamount ones.[32] $ZnCl_2$ is able to mix with QAS in molecular level to form complex with merit of lowing melting point of QAS[33] which enables the reaction of QAS specie with other chemicals taking place under moderate conditions. If QAS/$ZnCl_2$ complex is incorporated into polymer matrix through polymerization, the $ZnCl_2$ would be dispersed homogeneously in the matrix even with the anticipation of molecular level. The complex should show many

advantages over the physical composites, in which the inorganic compound dispersed heterogeneously.

In this work, we synthesized a poly(urethane) ionene/zinc chloride (PUI/$ZnCl_2$) complex through polymerization of poly(ethylene glycol), 1,4-butanediol and 4,4'-diphenylmethane diisocyanate with QAS/$ZnCl_2$ complex, and characterized the PUI/$ZnCl_2$ complex with NMR, intrinsic viscosity, TGA, POM, DSC, and tensile test. Furthermore, the antibacterial properties of the PUI/$ZnCl_2$ complex were investigated in detail. To our best knowledge, no paper has been published on the AB property of the complex of polyurethane ionene and zinc chloride. The complex with antibacterial property may find potential application in special areas such as medical device surfaces, telephone handset, children's toy, etc.[1-3, 34] This work provided a new way of synthesizing the polymeric ionene with antibacterial property plus other improved properties.

2. Experiment Section

2.1 Materials

N',N',N,N-tetramethyl-1,6-hexamethylenediamine (TMHDA) was purchased from J&k Scientific Ltd. 4,4'-diphenylmethane diisocyanate (MDI), 3-chloropropanol and poly(ethylene glycol) with M_n=4000g/mol (PEG4000) were purchased from Alfa Aesar Corp. (USA). MeOH, 1,4-butanediol (BDO) and *N,N*-dimethylformamide (DMF) purchased from Kelong Chemical Corp. (Chendu, China) were dried over calcium hydroxide and distilled before use. The PEG4000 procured from Alfa Aesar Corp. (USA) was first dissolved in the chloroform, and then washed by pure water three times, finally dried in a vacuum at 120 °C

for at least 4h before use. *Escherichia coli* (*E. coli* PTCC 1330) as gram-negative bacteria and *Staphylococcus aureus* (*S. aureus* PTCC 1112) as gram-positive bacteria were cultured in our own laboratory. Other chemical regents were all purchased from Kelong Corp. (Chengdu, China) and used as received.

2.2 Synthesis of 1,6-Bis(*N'*,*N*-dimethyl-3-hydroxylpropyl) Ammonium Chloride (BQAC-diol)

17.2g *N'*,*N'*,*N*,*N*-tetramethyl-1,6-hexamethylenediamine and 20.8g 3-chloropropanol with the molar ratio of (1:2.2) were added to a two-necked round-bottomed flask equipped with a condenser and nitrogen inlet, then 100mL distilled MeOH was added to the flask through condenser. The reaction was carried out at 80 °C[35] with a Teflon magnetic stirrer inside. After 24h, the MeOH was removed and the slight yellow product was appeared. Then the product was washed by excess acetone to remove the unreacted raw materials and residual MeOH. The final product was obtained by dried in vacuum.

2.3 Preparation of BQAC-Zn-diol

A mixture of the 1,6-bis(*N'*,*N*-dimethyl-3-hydroxylpropyl) ammonium chloride and zinc chloride in the molar radio (1:2) was added into one-neck round-bottomed flask and heat up to 120 °C with gentle stirring until a clear transparent yellow liquid formed.[33]

2.4 Synthesis of PUI/$ZnCl_2$ Complex

PUI/$ZnCl_2$ complex was synthesized by one-step melting polymerization from PEG4000, MDI, BDO, and BQAC-Zn-diol. The feed ratios are shown in Table 1. The reaction was allowed at 120 °C under nitrogen atmosphere until the product was creeping. After that (~1h), the product was dissolved in DMF and then casted onto Teflon plate to get films for later

characterization. Solvent was first evaporated at 60 °C for two days, and then placed in a vacuum oven at 30 °C until constant weight was obtained.

2.5 Intrinsic viscosity

Intrinsic viscosities were determined at a concentration of 40mg/25mL (w/v) using Ubbelohde viscometers at 25 °C in DMF. The intrinsic viscosity values were calculated by Solomon-Ciuta equation.

$$\sqrt{2(\eta_{sp} - \ln \eta_r)} / C$$

2.6 Nuclear Magnetic Resonance (NMR)

^{1}H-NMR spectra for BQAC-diol and PUI/$ZnCl_2$ were recorded with a Brucker AC-P 400 MHz spectrometer and performed at ambient temperature in water (D_2O) and dimethyl sulfoxide (DMSO) respectively, using tetramethylsilane as internal chemical.

2.7 Atomic Absorption Spectrophotometry (AAS)

The Zn element was detected by atomic absorption spectrometer (Spectr AA 220FS, USA). The 0.5 g sample was first dissolved in 5 mL concentrated nitric acid and 1 mL perchloric acid mixture by heating until the transparent solution was obtained. And then the solution was diluted to 100mL before testing.

2.8 Thermo Gravimetric Analysis (TGA)

The thermal stability of PUI/$ZnCl_2$ was evaluated by thermogravimetric analysis on the TG 209 F1 (NETZSCH, Germany). 5-10 mg samples were analyzed over the temperature range of 40-700 °C at a heating rate of 10 °C/min under N_2 atmosphere.

2.9 Differential Scanning Calorimetry (DSC)

DSC analysis was carried out on a TA instrument DSC-Q200. Samples were quickly heated

to 140 °C, and maintained for 5 min to eliminate thermal history, then quenched to -70 °C with liquid nitrogen, and then heat to 140 °C at the rate of 10 °C/min, and finally cooled to -60 °C at the same rate. Both heating and cooling scans were recorded for analysis.

2.10 Polarized Optical Microscopy (POM)

The spherulitic morphologies and growth rate of PUI/$ZnCl_2$ were investigated with a polarized optical microscope (POM) (NIKON ECLIPSE LV100POL). The sample films were prepared between two microscopic cover glasses at 160 °C. All the samples were first melted on a hot stage (HSC621V) at 60 °C for 3 min to eliminate the thermal history and quenched to 20 °C to observe the spherulitic growth. The growth rate (G) was calculated from the slopes of the plots of spherulitic radii versus crystallization time.

2.11 Scanning Electron Microscopy (SEM)

The morphology of the fractured surfaces of specimens was observed by scanning electron microscope (SEM, XL-30s, FEG, Philips, Holland) with an accelerating voltage of 5 kV. The samples were first fractured in the liquid nitrogen, and then fractured surface was sputtered with a layer of gold before observation.

2.12 Antibacterial Test

The AB activity was checked against *S. aureus*, a gram-positive bacterium, and *E. coli*, a gram-negative bacterium, according to the agar-well diffusion method (Kavanagh et al., 1963).[36] In this method, first, holes were cut in the agar by means of a sharp 5mm cork borer, and then stock solutions of different PUI/$ZnCl_2$ samples in the concentration of 100mg/mL were prepared in DMSO and added to the holes. At the same time, the small molecular monomers whose molar weight was equal to ionic unit content of the sample

PUI-10.5/Zn-7.9, were also added in the respective hole. Finally, the results of all were compared with the commercial AB drug i.e., triclosan, the standard drug and DMSO were used as positive and negative control, respectively. The AB activity was determined by measuring the zone of inhibition of each sample.

2.13 Tensile test

Tensile strength and elongation at break of polymer films with a dog-bone shape were measured on a Universal Testing Machine (SANS CMT4104, SANS Group, China) at a crosshead speed of 50 mm/min at room temperature. The thickness and width of the specimens were 0.5 mm and 5 mm, respectively. The length of the sample between the two mechanical grips of Testing Machine was 10 mm. Five measurements were conducted for each sample, and the results were averaged to get a mean value.

3. Results and Discussion

3.1 Synthesis of BQAC-Zn-diol and PUI/$ZnCl_2$ complex

$ZnCl_2$ is an inorganic salt usually showing bad compatibility with organic polymers. It is difficult to incorporate it into polymer matrix to form complex through simple blending so as to introduce antibacterial activity. Quaternary ammonium salts were reported to be form complex with $ZnCl_2$ via simple mixing.[33] The melting point of quaternary ammonium salts could be reduced significantly through the formation of complex. Quaternary ammonium cation also showed antibacterial activity in some cases as mentioned above.[12,21] In order to incorporate $ZnCl_2$ into polymer matrix, we synthesized a quaternary ammonium salts diol and mixed it with $ZnCl_2$ to form a complex chain-extender. $ZnCl_2$ can be easily incorporated into

polyurethane matrix by polymerization of polyols, diisocyanates, and the complex chain-extender.

In this study, quaternary ammonium salt diol, i.e., 1,6-bis(*N',N*-dimethyl-3-hydroxylpropyl) ammonium chloride (BQAC-diol), was synthesized from Menschutkin reaction of TMHDA and 3-chloropropanol in MeOH, as shown in Scheme 1. After purification, slightly yellow powdered products were obtained, which is moisture sensitive and has a melting point of about 180 °C. The chemical structure of BQAC-diol was characterized by ^{1}H-NMR spectrum, as shown in Fig. 1. The peaks at 3.03 ppm (δH^k), 3.32 ppm (δH^j) and 3.25 ppm (δH^l) were assigned to methyl or methylene groups which were attached directly to the quaternary ammonium atom. The peaks at 1.82 ppm (δH^i), 1.68 ppm (δH^m) and 1.34 ppm (δH^n) were ascribed to methylene groups. The complex chain-extender was prepared by mixing BQAC-diol with $ZnCl_2$ at 120 °C until formation of a transparent and homogenous melt for about 2 h with the aid of mechanical stir. The reaction is shown as follows:

$$QCl+ZnCl_2=Q^+[ZnCl_3]^-$$

where Q^+ represents the quaternary ammonium cation. It is interesting to find that the melting point of the complex chain-extender was reduced to about 100 °C, compared to 180 °C for BQAC-diol. Such a reduction was ascribed to the decreased interaction between the formed $[ZnCl_3]^-$ and the quaternary ammonium due to the increased anion size by formation of $[ZnCl_3]^-$,[33] and would facilitate polymerization for preparation of PUI/$ZnCl_2$ complex.

PUI/$ZnCl_2$ complex was prepared by chain-extension reaction of 1,4-butanediol, MDI, PEG4000 and BQAC-Zn-diol, as shown in Scheme 2. A series of PUI/$ZnCl_2$ complex with

different contents of quaternary ammonium cation and $ZnCl_2$ were synthesized and their intrinsic viscosities were shown in Table 1. Gel permeation chromatography had not been carried out since ionic interactions with the column can occur during elution.[37] The intrinsic viscosity of PUI/$ZnCl_2$ complex increased gradually with increasing BQAC-Zn-diol. The $ZnCl_2$ in BQAC-Zn-diol might catalyze the chain-extension reaction like some other Lewis acid catalysts such as dibutyltin dilaurate, since the chain-extension reaction of the reactants containing $ZnCl_2$ took place much faster than that without $ZnCl_2$. The contents of Zn^{2+} in the complexes were analyzed by atomic absorption spectrophotometry, and the results are listed in Table 1. It can be seen that the contents of Zn^{2+} obtained via atomic absorption spectrophotometry (experimental) were very close to the values in feed (theoretical).

The chemical structure of PUI/$ZnCl_2$ complex was characterized by ^{1}H-NMR. Fig. 2 showed the ^{1}H-NMR spectra of PUI-0/Zn-0 and typical PUI-10.5/Zn-7.9 complex. PUI-0/Zn-0 contained no ionic unit and was prepared from PEG, BDO and MDI. The signal at 3.51 ppm (δH^a) was ascribed to the methylene protons of soft PEG segment, those occurring at 4.10 ppm (δH^f), and 1.70 ppm (δH^g) were ascribed to the methylene protons of two different methylene protons of BDO specie, and the signals for two different benzene protons and methylene protons of MDI unit were found at 7.36 ppm (δH^c), 7.08 ppm (δH^d), and 3.78 ppm (δH^e), respectively. In addition, the nitrogen proton of the urethane linkage could also be seen at 9.55 ppm (δH^b). Besides all the proton signals of PUI-0/Zn-0, the signals belonging to BQAC-diol, i.e., 1.34 ppm (δH^n), 1.82 ppm (δH^i), 1.68 ppm (δH^m), 3.03 ppm (δH^k), could also be obviously observed on the spectrum of the typical PUI-10.5/Zn-7.9 complex except peaks at 3.32 ppm (δH^j), and 3.25 ppm (δH^l) which were overlapped by peak

at 3.51 ppm (δH^a). In addition, the peak at 3.50 ppm (δH^h) was shifted to 4.16 ppm after polymerization. The results indicated successful synthesis of PUI/$ZnCl_2$ from PEG, BDO, MDI, and BQAC-Zn-diol.

3.2 Thermal stability of PUI/$ZnCl_2$ complex

The thermal stability of PUI/$ZnCl_2$ complex was investigated by TGA. Fig. 3 showed the TGA curves of the samples. It was clear that thermal degradation of the complex mainly occurred in two steps: the first step was ascribed to the degradation of the hard segment at around 308 °C, and the second step was attributed to the thermal decomposition of soft segment at around 400 °C.[38] For the effect of ionic content on the thermal stability of the samples, we found that the maximum thermal decomposition temperature (T_{max}) for the first step of all sample was around 308 °C, suggesting that the incorporation of ionic unit could not apparently change the thermal stability of hard segment of the PUI/$ZnCl_2$ complex. The T_{max} for the second step decreased gradually with increasing ionic content, indicating a gradually deteriorative thermal stability of the soft segment, which might be ascribed to the presence of $ZnCl_2$, which may act as a catalyst for thermal decomposition of PEG soft segment. In order to prove this conclusion, we measured the thermal stability of PUI-10.5/Zn-0, which was obtained from PUI-10.5/Zn-7.9 by removal of $ZnCl_2$ through dialysis with water. The T_{max} for the second step decomposition of PUI-10.5/Zn-0 was improved by about 20 °C with the value of 402.8 °C, compared to 382.0 °C for PUI-10.5/Zn-7.9. Although the thermal stability of PUI/$ZnCl_2$ complex deteriorated with increasing ionic content, it was worth noting that the deteriorative extent was in an acceptable

range which would not affect the thermal processing of the resulting materials, since the maximum decreasing extent of the second step T_{max} between PUI-0/Zn-0 and other PUI/$ZnCl_2$ was only less than 25 °C. The values for PUI-0/Zn-0 was 405.2 °C and decreased gradually to 403.2, 396.8, 388.5, 383.4 and 382.0 °C for PUI-1.7/Zn-1.3, PUI-4.0/Zn-3.0, PUI-6.3/Zn-4.7, PUI-8.6/Zn-6.4 and PUI-10.5/Zn-7.9, respectively.

3.3 Thermal transition and crystallization behavior of PUI/$ZnCl_2$ complex

The thermal transition and crystallization behavior of PUI/$ZnCl_2$ was characterized by DSC. Fig. 4 showed the DSC scans of PUI/$ZnCl_2$ complex, and the corresponding data are summarized in Table 2. From the heating scans (Fig. 4a), we can see that all the samples showed only one glass transition, one cold crystallization peak if detectable and one melting peak. The presence of one glass transition indicated that the soft and the hard segments were miscible irrespective of the compositions. It was worth noting that the glass transition temperature (T_g) of PUI/$ZnCl_2$ complex decreased gradually with increasing ionic content. The T_g value was -38.29 °C for PUI-0/Zn-0 and decreased gradually to -43.43, -45.97, -50.31 and -54.70 °C for PUI-1.7/Zn-1.3, PUI-4.0/Zn-3.0, PUI-6.3/Zn-4.7 and PUI-8.6/Zn-6.4, respectively. The T_g of PUI-10.5/Zn-7.9 might be lower than -54.70 °C according to the changing trend, but it was not observed due to the complete crystallization during quenched process, as discussed later. It is generally accepted that the T_g of polymer should increase by the incorporation of ionic unit,[39-41] since electrostatic interaction caused by the ionic unit could decrease the chain mobility. But T_g not increased but decreased with incorporation and increasing content of ionic unit, which might be ascribed to the fact that the content of MDI

was reduced with increasing the complex chain-extender, since the molecular weight of the complex chain-extender was much higher than that of BDO, which would decrease the rigidity of the hard segment, i.e., making the polymer chain more flexible, thus lead to a reduction in $T_{g.}$.

For the effect of ionic unit content on the crystallization ability of the PUI/$ZnCl_2$ complexes, we can see that the cold crystallization peak also shifted to lower temperature range with increasing ionic unit content, suggesting an increased crystallizability. It was worth noting the crystallization was arisen from PEG soft segment although the hard segment may affect the crystallizability of the soft segment by affecting the chain mobility. The cold crystallization peak temperature (T_{cc}) was 3.85 ℃ for PUI-0/Zn-0, which decreased significantly to -10.82, -23.71, -34.37 and -43.73 ℃ for PUI-1.7/Zn-1.3, PUI-4.0/Zn-3.0, PUI-6.3/Zn-4.7 and PUI-8.6/Zn-6.4, respectively. The cold crystallization of PUI-10.5/Zn-7.9 was not observed due to the rapid crystallization of the sample even under quenching. The lower T_{cc} usually represents higher crystallization rate. That is to say, the crystallization rate of the complex increased with increasing ionic unit content, which should also relate to the increased flexibility of the polymer chain, since the flexible chain was easier to fold into crystal lattice than the hard chain during crystallization, which would cause an increased crystal growth rate. The melt crystallization behavior of the complexes was also investigated from the cooling scans (Fig 4b), and similar results were obtained. Except for flexibility, another factor that increased nucleation efficiency by the aggregation of ionic unit containing hard segment may also increase the crystallization rate of polyurethane ionenes.[39,42] In addition, $ZnCl_2$ if dispersed as particle may also act as nucleation site for crystallization of

the complexes. In order to confirm which factor responded for the accelerated crystallization rate of the complexes, the crystalline morphology and spherulitic growth rate of the samples would be further investigated in the following text. In addition, we can find that the cold crystallization enthalpy decreased gradually with increasing ionic unit content, which must be attributed to the inevitable partial crystallization during quenching process.

Both the melting peak temperature (T_m) and the fusion enthalpy (ΔH_m) showed uptrend with increasing ionic unit content. The T_m value for PUI-0/Zn-0 was 39.12 °C, and those for PUI-1.7/Zn-1.3, PUI-4.0/Zn-3.0, PUI-6.3/Zn-4.7, PUI-8.6/Zn-6.4 and PUI-10.5/Zn-7.9 were 39.04, 41.32, 42.45, 44.32, and 46.76 °C, respectively, ΔH_m values for PUI-0/Zn-0, PUI-1.7/Zn-1.3, PUI-4.0/Zn-3.0, PUI-6.3/Zn-4.7, PUI-8.6/Zn-6.4 and PUI-10.5/Zn-7.9 were 36.95, 35.43, 46.93, 47.87, 52.89 and 57.66 J/g, respectively. Such a change should be ascribed to the increased crystallizability of the complex with increasing ionic unit content, since more perfect crystals with high thermal stability and degree of crystallinity should be formed with increased crystallizability.

As the above mentioned that to find which factor accounted for the increased crystallization rate of the complex with increasing ionic unit content, the crystalline morphology and spherulitic growth rate of the complex were characterized by POM. Both the nucleation density and spherulitic growth rate, which are the two aspects of crystallization rate, can be obtained with POM. Fig. 5 showed the crystalline morphologies of the PUI/$ZnCl_2$ complexes after isothermally crystallized at 20 °C. The nucleation density did not change apparently with the complex composition, suggesting that the presence of both ionic interaction and $ZnCl_2$ could not lead to increased nucleation density. The increased

crystallization rate must be resulted from the increased spherulitic growth rate (G), which was calculated from the slopes of the plots of spherulitic radii versus crystallization time. Fig 6 showed the G values of PUI/$ZnCl_2$ complexes. PUI-0/Zn-0 showed a G of only 0.095 μm/s at 20 °C, and the G values increased gradually to 0.151, 0.158, 0.371, 0.668 and 0.852 μm/s for PUI-1.7/Zn-1.3, PUI-4.0/Zn-3.0, PUI-6.3/Zn-4.7, PUI-8.6/Zn-6.4 and PUI-10.5/Zn-7.9, respectively.

3.4. Phase morphology of PUI/$ZnCl_2$ complex

The phase morphology of PUI/$ZnCl_2$ complex was studied by SEM. Fig. 7 shows the SEM micrographs for cryo-fractured surfaces of PUI-0/Zn-0 and some PUI/$ZnCl_2$ complexes. No phase-separation can be observed, which further confirmed that the soft segment and hard segment of the samples were miscible, in consistent with the presence of a single T_g as detected by DSC. The reason might be ascribed to the presence of the ether oxygen atoms of the PEG, which can stabilize the ions[43] and consequently, to some extent, prevent the phase separation. It is worth noting that all the samples showed homogeneous phase morphology regardless of the content of $ZnCl_2$, which indicate that no aggregation of $ZnCl_2$ took place and it dispersed in PUI matrix at molecular level, ascribing to the complexation between $ZnCl_2$ and QAS specie.

3.5 Antibacterial property of PUI/$ZnCl_2$ complex

During antibacterial (AB) property measurement, we found that the prepared films tended to curl on the surface of the solid agar, which would affect the accuracy of the results. Therefore,

the cylinder plate procedure was used to measure the antibacterial properties, as described in experiment section. In this method, a clear transparent zone of inhibition occurred around the sides of test hole after incubation if the studied bacterial was killed by the specimen. DMSO was used as the solvent, since it showed no antibacterial activity for both *S. aureus* and *E. coli*. Fig. 8 showed the digital photos for inhibition zone of PUI/$ZnCl_2$ complexes against *E. coli* after 48h incubation. It can be seen that PUI-0/Zn-0, without ionic unit, did not display any antibacterial activity since no inhibition zone can be observed. The inhibition zone appeared after incorporation of ionic unit and the diameters of inhibition zones increased gradually with increasing ionic content, indicating enhanced AB activity. Similar phenomenon was also observed in the case of *S. aureus* as the bacterial. For brevity, the digital photos were not shown. The diameters of inhibition zones for AB activity of PUI/$ZnCl_2$ complexes against both *E. coli* and *S. aureus* at 48 h were shown in Fig. 9. No obvious difference between the AB effects on the both bacteria could be obtained. We can summarize that the PUI/$ZnCl_2$ complexes were able to inhibit the growth of both gram-positive and gram-negative bacterium. It was difficult to compare between different cultures as there were many unknown factors which could cause large deviation in the test, and cylinder-plate cultures were highly sensitive to the density and growth phase of colony.[28]

It was worth noting that the PUI/$ZnCl_2$ complexes contained two species that might have AB activity, i.e., quaternary ammonium and $ZnCl_2$. In order to prove which one provided the complex with AB property, we investigated the effect of $ZnCl_2$ content on the AB activity of the complexes. PUI/$ZnCl_2$ complexes with same quaternary ammonium content and three different $ZnCl_2$ contents were employed. PUI-10.5/Zn-0 with no $ZnCl_2$ was prepared by

dialysis of PUI-10.5/Zn-7.9, and PUI-10.5/Zn-14.6 was prepared with BQAC-Zn-diol, consisting of BQAC-diol and $ZnCl_2$ with the molar radio of 1:4, as a chain-extender. The results were listed in Table 3. PUI-10.5/Zn-0 showed no AB activity, indicating that the PUI had no AB activity although containing quaternary ammonium. Several studies have shown that QAS with alkyl chain lengths less than eight carbon atoms have no AB activity,[44,45] the same thing also happened to the polymer ionenes. It is because the QAS surface creates strong electrostatic interaction with bacteria and then the hydrophobic alkyl chain diffuses through the cell wall and disrupts the membrane, causing cell death. Thus, if the alkyl chain is too short or hydrophilic, then the cell can survive from the contact of QAS even though electrostatic force still exists. The diameter of inhibition zones increased gradually with $ZnCl_2$ content regardless of the kind of bacterial. We can conclude that the AB activity of the PUI/$ZnCl_2$ complexes was ascribed to the presence of $ZnCl_2$. The AB activity of $ZnCl_2$ and BQAC-diol solutions with the same concentration as that in PUI-10.5/Zn-7.9 was also investigated. BQAC-diol showed no while $ZnCl_2$ showed good AB activities. By comparing the AB activity among $ZnCl_2$, BQAC-diol and PUI/$ZnCl_2$, we could conclude that synergistic effect between $ZnCl_2$ and BQAC-diol may take place since the diameter of PUI-10.5/Zn-7.9 containing both $ZnCl_2$ and BQAC-diol showed larger diameter of inhibition zone than $ZnCl_2$ solution.

From Table 3, no inhibition zone was observed for term 5 against both of studied bacteria, which meant the monomer BQAC-diol in this study showed no AB behavior. To probe the AB function of zinc ion further, agar diffusion results showed that AB activity of PUI-10.5/Zn-14.6 was better than that of corresponding PUI-10.5/Zn-7.9 at 48h. But this

trend was not obvious or even opposite when the testing time was longer, because from Fig. 10, it was clearly found that inhibition zone of PUI-10.5/Zn-7.9 was larger than that of PUI-10.5/Zn-14.6 after 72 h. The low molecular weight agent commonly used was more likely to migrate toward the surface than the high molecular weight one during use,[46] so the AB effect of PUI/$ZnCl_2$ containing high ionic content was weakened by migration of $ZnCl_2$, which explained why there were double inhibition rings seen in the agar plate when the $ZnCl_2$ content was too high (Fig. 8c). The outside semi-transparent one would be caused by the diffusion of $ZnCl_2$ since the *E. coli* was not completely killed in this zone. Thus except thermal stability, high $ZnCl_2$ content could also lower AB durability, even though it might bring the high efficient AB property at the same time.

The effect of incubation time on the AB activity of PUI/$ZnCl_2$ complexes was investigated and compared with that of a broad-spectrum antibacterial, i.e., triclosan. The results were listed in Fig.10. It cannot be ignored that the PUI/$ZnCl_2$ complexes were not as efficient as triclosan at the beginning of the test, but with the measurement prolonging, the inhibition zones of complexes increased gradually, while zone of triclosan remained almost the same within the measurement error. After 96h, the sample PUI-10.5/Zn-7.9 showed larger zone than triclosan, indicating better AB property.

3.6 Mechanical properties of PUI/$ZnCl_2$ complex

The mechanical properties are very important for practical application of materials. Therefore, the mechanical property of PUI/$ZnCl_2$ was characterized and the results are shown in Fig. 11. From the stress-strain curves (Fig 11a), when can see that all the samples showed a typical

behavior of semi-crystalline thermoplastic polyurethane with yielding, relatively low tensile strength and high elongation at break. The PUI/$ZnCl_2$ complexes showed higher yield strength and tensile strength than PUI-0/Zn-0, which might be ascribed to the strengthening effect of the ionic unit via physical crosslinking, and the increased intrinsic viscosity by the incorporation of complex chain-extender would also constitute partial reason for the strength. The elongation at break of all the samples was over 1000% and an uptrend in the value of the elongation occurred with increasing ionic unit content, which was attributed to the increased chain flexibility and intrinsic viscosity of the complex, as discussed in Section 3.3.

4. Conclusions

Complex of gemini quaternary ammonium and zinc chloride was prepared and used as ionic chain-extender to synthesize PUI/$ZnCl_2$ complex through polymerization with MDI, PEG, and BDO. No phase-separation occurred for the PUI/$ZnCl_2$ complex regardless of the composition, and $ZnCl_2$ was found to disperse in the PUI matrix at molecular level. The content of ionic chain-extender played an important role in the physical properties and antibacterial properties of the PUI/$ZnCl_2$ complex. With increasing ionic unit content, the thermal stability of the complex was slightly reduced, the glass transition temperature was significantly lowered, and the crystallization rate was dramatically accelerated. Both the reduction in T_g and the acceleration in crystallization rate were resulted from the improved flexibility of the complex. The accelerated crystallization rate was arisen by the significantly increased spherulitic growth rate. The melting point and fusion enthalpy also increased with increasing ionic unit content due to the improved crystallizability. The antibacterial test

suggested that the antibacterial activity of the complex was ascribed to the presence $ZnCl_2$, and the antibacterial capability increased with the content of $ZnCl_2$. Although QAS in PUI did not show any antibacterial activity, it can provide synergetic effect by complexation with $ZnCl_2$. The tensile test indicated that the mechanical properties of PUI/$ZnCl_2$ were better than that of the PU synthesized from PEG, MDI and BDO.

Acknowledgement

This work was supported by the National Science Foundation of China (51373107 and 51121001) and the Specialized Research Fund for the Doctoral Program of Higher Education (20110181130008).

References and Notes

[1] *Center for Degradable and Flame-Retardant Polymeric Materials (ERCPM-MoE), College of Chemistry, State Key Laboratory of Polymer Materials Engineering, National Engineering Laboratory of Eco-Friendly Polymeric Materials (Sichuan), Sichuan University, 29 Wangjiang Road, Chengdu 610064, China.*

[2] *College of Chemistry and Chemical Engineering, Southwest University, Beibei Chongqing 400715, China*

Email: jbzeng@swu.edu.cn; yzwang@scu.edu.cn; Fax/tel: +86-28-85410259.

(1) J. Hardes, H. Ahrens, C. Gebert, A. Streitbuerger, H. Buerger, M. Erren, A. Gunsel, C. Wedemeyer, G. Saxler, W. Winkelmann and G. Gosheger, *Biomaterials,* 2007, **28**, 2869–2875.

(2) V. Decraene, J.Pratten and M. Wilson, *Infect. Control Hosp. Epidemiol.,* 2008, **29**, 1181–1184.

(3) V. Decraene, J. Pratten and M. Wilson, *Curr. Microbiol.,* 2008, **57**, 269–273.

(4) M. Marini, S. De Niederhausern, R. Iseppi, M. Bondi, C. Sabia, M. Toselli and F. Pilati, *Biomacromelecules*, 2007, **8**, 1246-1254.

(5) C. Tang, W. Sun and W. Yan, *RSC. Adv.*, 2014, **4**, 523-530.

(6) X. Wang, Y. Dai, J. Zou, L. Meng, S. Ishikawa, S. Li, M. Abuobeidah and H. Fu, *RSC Adv.*, 2013, **3**, 11751-11758.

(7) A. D. Russell and W. B. Hugo, *Prog. Med. Chem.,* 1994, **31**, 351-370.

(8) K. R. Raghupathi, R. T. Koodali and A. C. Manna, *Langmuir*, 2011, **27**, 4020-4028.

(9) C. M. Jones and E. M. V. Hoek, *J. Nanopart. Res*., 2010, **12**, 1531-1551.

(10) R. O. Darouiche, *Clin. Infect. Dis.,* 2003, **36**, 1284–1289.

(11) H. Gollwitzer, P. Thomas, P. Diehl, E. Steinhauser, B. Summer, S. Barnstorf, L. Gerdesmeyer, W. Mittelmeier and A. Stemberger, *J. Orthop. Res.,* 2005, **23**, 802–809.

(12) S. Lin, J. Wu, H. Jia, L. Hao, R. Wang and J. Qi, *RSC Adv.*, 2013, **3**, 20758-20764.

(13) H. Wang, C. V. Synatschke, A. Raup, V. Jerome, R. Freitag and S. Agarwal, *Polym.Chem.*, 2014, **5**, 2453-2460.

(14) I. Ahmad, J. H. Zaidi, R. Hussain and A. Munir, *Polym. Int.,* 2007, **56**, 1521–1529.

(15) L. Wang, X. Yang, H. Chen, G. Yang, T. Gong, W. Li and S. Zhou, *Polym. Chem.,* 2013, **4**, 4461-4468.

(16) A. H. M. M. El-Sayed, W. M. Mahmoud, E. M. Davis and R. W. Coughlin, *Int. Biodeterior. Biodegrad.,* 1996, **37**, 69–79.

(17) X. Y. Ma and W. D. Zhang, *Polym. Degrad. Stabil.,* 2009, **94**, 1103-1109.

(18) Y. Xue, Y. Pan, H. Xiao and Y. Zhao, *RSC Adv.*, 2014, **4**, 46887-46895.

(19) E. R. Kenawy, S.D. Worley and R. Broughton, *Biomacromolecules*, 2007, **8**, 1359–1384.

(20) A. Yari, H. Yeganeh and H. Bakhshi, *J. Mater. Sci.: Mater. Med.*, 2012, **23**, 2187-2202.

(21) R. R. Pant, P. A. Fulmer, M. B. Harney, J. P. Buckley and J. H. Wynne, *J. Appl. Polym. Sci.,* 2009, **113**, 2397–2403.

(22) R.R. Pant, B.T. Rasley, J. P. Buckley, C. T. Lloyd, R. F. Cozzens, P. G. Santangelo and J. H. Wynne, *J. Appl. Polym. Sci.,* 2007, **104**, 2954-2964.

(23) R. R. Pant, J. L. Buckley, P. A. Fulmer, J. H. Wynne, D. M. McCluskey and J. P. Phillips, *J. Appl. Polym. Sci.,* 2008, **110**, 3080-3086.

(24) O. Jaudouin, J. J. Robin, J. M. L. Cuesta, D. Perrin and C. Imbert, *Polym. Int.,* 2012, **61**, 495-510.

(25) Y. Zhu, J. Hu and K. Yeung, *Acta Biomaterialia*, 2009, **5**, 3346-3357.

(26) T. Ikeda, H. Yamaguchi and S. Tazuke, *J. Bioact. Compat. Polym.,* 1990, **5**, 31-41.

(27) T. Tashiro, *Macromol. Mater. Eng.*, 2001, **286**, 63-87.

(28) D. Boyd, H. Li, D. A. Tanner, M. R. Towler and J. G. Wall, *J. Mater. Sci,: Mater. Med.*, 2006, **17**, 489-494.

(29) R. Jayakumar, M. Rajkumar, R. Nagendran and S. Nanjundan, *J. Appl. Polym. Sci.,* 2002, **85**, 1194-1206.

(30) R. Kumar, S. Howdle and H. Munstedt, *J. Biomed. Mater. Res.,* 2005, **75B**, 311-319.

(31) J. S. Park, J. Kuang, H. J. Gwon, Y. M. Lim, S. I. Jeong, Y. M. Shin, M. S. Khil and Y. C. Nho, *Radiat. Phys. Chem.*, 2013, **88**, 60-64.

(32) K. R. Raghupathi, R. T. Koodali and A. C. Manna, *Langmuir*, 2011, **27**, 4020-4028.

(33) A. P. Abbott, G.. Capper, D. L. Davies and R. Rasheed, *Inorg. Chem.*, 2004, **43**, 3447-3452.

(34) J. H. Wynne, P. A. Fulmer, D. M. McCluskey, N. M. Mackey and J. P. Buchanan, *ACS Appl. Mater. Interfaces*, 2011, **3**, 2005-2011.

(35)S. R. Williams, E. M. Borgerding, J. M. Layman, W. Wang, K. I. Winey and T. E. Long, *Macromolecules*, 2008, **41**, 5216-5222.

(36) M. Nisar, W. A. Kaleem, M. Qayum, I. K. Marwat, M. Z. U. Haq, I. Ali and M. I. Choudhary, *Pak. J. Bot.*, 2011, **43**, 311-317.

(37) W. Siebourg, R. Lundberg, R. Lenz and K. C. Frisch, *Macromolecules,* 1980, **13**, 1013-1016.

(38) Z. S. Petrovic, Z. Zavargo, J. H. Flyn and W. J. Macknight. *J. Appl. Polym. Sci.,* 1994, **51**, 1087–1095.

(39) J. B. Zeng, F. Wu, C. L. Huang, Y. S. He and Y. Z. Wang, *ACS Macro Lett*, 2012, **1**, 965-968.

(40) B. Kim, J. Yang, S. Yoo and J. Lee, *Colloid. Polym. Sci.,* 2003, **281**, 461-468.

(41) S. Mondal and J. L. Hu, *J. Membr. Sci.,* 2006, **274**, 219-226.

(42) F. Wu, C. L. Huang, J. B. Zeng, S. L. Li and Y. Z. Wang, *Polymer*, 2014, **55**, 4358-4368.

(43) S. Dou, S. Zhang, R. J. Klein, J. Runt and R. H. Colby, *Chem. Mater.*, 2006, **18**, 4288-4295.

(44) X. Liu, H. Zhang, Z. Tian, A. Sen and H. R. Allcock, *Polym. Chem.*, 2012, **3**, 2082-2091.

(45) E. Tomlinson, M. R. W. Brown and S. S. Davis, *J. Med. Chem.,* 1977, **20**, 1277-1282.

(46) M. Colonna, C. Berti, E. Binassi, M. Fiorini, S. Sullalti, F. Acquasanta, M. Vannini, D. D. Gioia and I. Aloisio, *Polymer*, 2012, **53**, 1823-1830.

Tables and Figures

Table 1. Compositions and intrinsic viscosities of PUI/$ZnCl_2$ Complexes.

Sample	Molar ratio	Zn^{2+} content (%)		[η]
	PEG/BQAC-Zn-diol/BDO/MDI	Theoretical	Experimental	(dL/g)
PUI-0/Zn-0	1/0/4.30/5.30	0	0	0.68
PUI-1.7/Zn-1.3	1/0.27/3.60/4.87	0.61	0.67±0.11	0.97
PUI-4.0/Zn-3.0	1/0.63/2.67/4.30	1.43	1.50±0.09	1.11
PUI-6.3/Zn-4.7	1/0.99/1.73/3.72	2.26	2.09±0.07	1.19
PUI-8.6/Zn-6.4	1/1.35/0.79/3.14	3.07	2.95±0.12	1.32
PUI-10.5/Zn-7.9	1/1.66/0/2.66	3.78	3.09±0.11	1.69

Table 2. Thermal transition, crystallization and melting behaviors PUI/$ZnCl_2$ complexes.

Sample	T_g (°C)	T_{cc} (°C)	ΔH_{cc} (J/g)	T_m (°C)	ΔH_m (J/g)	T_{mc} (°C)	ΔH_{mc} (J/g)
PUI-0/Zn-0	-38.29	3.85	34.19	39.12	36.95	---	---
PUI-1.7/Zn-1.3	-43.43	-10.82	22.14	39.04	35.43	---	---
PUI-4.0/Zn-3.0	-45.97	-23.71	24.12	41.32	46.93	---	---
PUI-6.3/Zn-4.7	-50.31	-34.37	14.30	42.45	47.87	-5.93	40.66
PUI-8.6/Zn6.4	-54.70	-43.73	13.14	44.32	52.89	4.77	51.59
PUI-10.5/Zn-7.9	---	----	----	46.76	57.66	10.50	54.22

Table 3. The influence of $ZnCl_2$ content on antibacterial activity of PUI/$ZnCl_2$ at 48h.

Term	Sample	solution	Concentration (mg/mL)	Diameter of inhibition zone (mm)	
				E.coli	*S.aureus*
1	PUI-10.5/Zn-0[a]	DMSO	100/1	0	0
2	PUI-10.5/Zn-7.9	DMSO	100/1	15.76±1.05	17.44±1.81
3	PUI-10.5/Zn-14.6[b]	DMSO	100/1	17.59±1.28	20.92±0.81
4	$ZnCl_2$	H_2O	7.9/1[c]	11.10±0.53	11.44±1.10
5	BQAC-diol	H_2O	10.5/1[c]	0	0

[a] Prepared by dialysis of PUI-10.5/Zn-7.9;

[b] Synthesized with the other BQAC-Zn-diol prepared by mixing BQAC-diol and $ZnCl_2$ with the molar ratio of 1:4;

[c] The content was equal to ionic molar content of PUI-10.5/Zn-7.9.

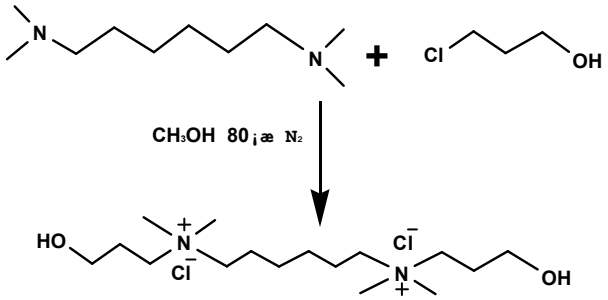

Scheme 1. Synthesis of 1,6-bis(*N',N*-dimethyl-3-hydroxylpropyl) ammonium chloride.

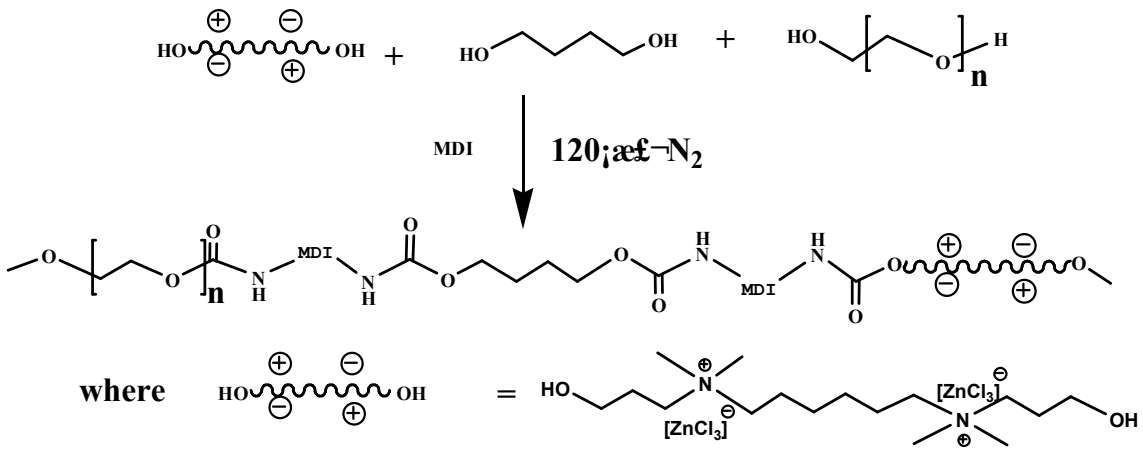

Scheme 2. Synthesis of PUI/$ZnCl_2$ complex.

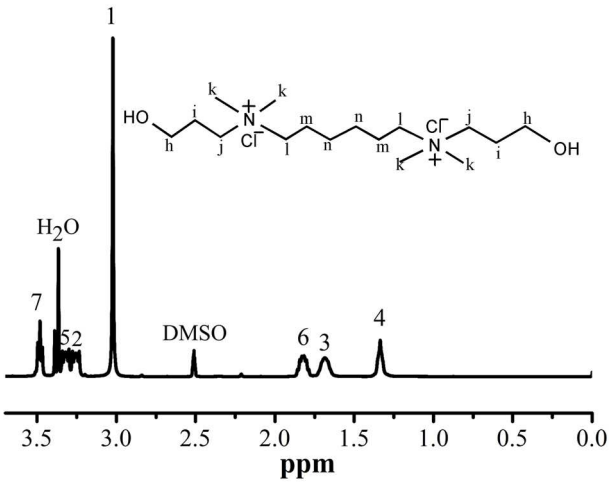

Fig. 1. [1]H-NMR spectrum of 1,6-bis(*N',N*-dimethyl-3-hydroxylpropyl) ammonium chloride.

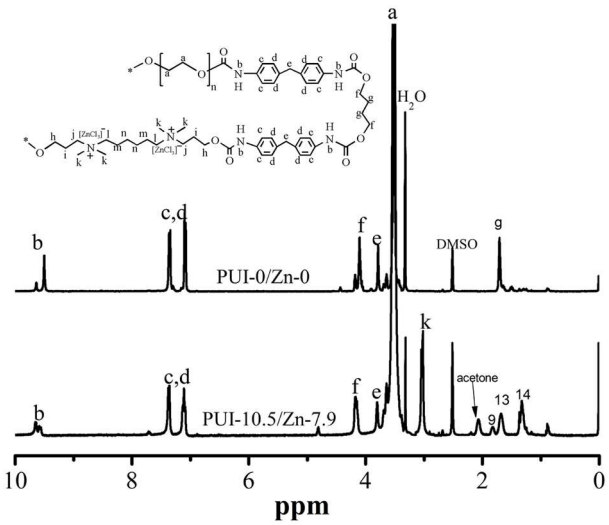

Fig. 2. ^{1}H-NMR spectra of PUI-0/Zn-0 and typical PUI/$ZnCl_2$ complex.

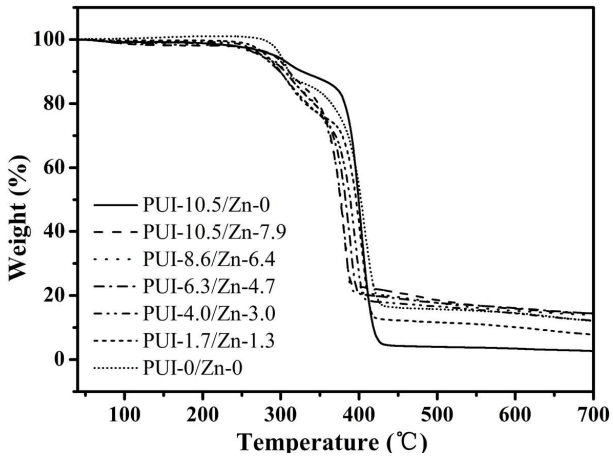

Fig. 3. TG curves of PUI/$ZnCl_2$ complexes at a heating rate of 10 °C min^{-1} under N_2 atmosphere.

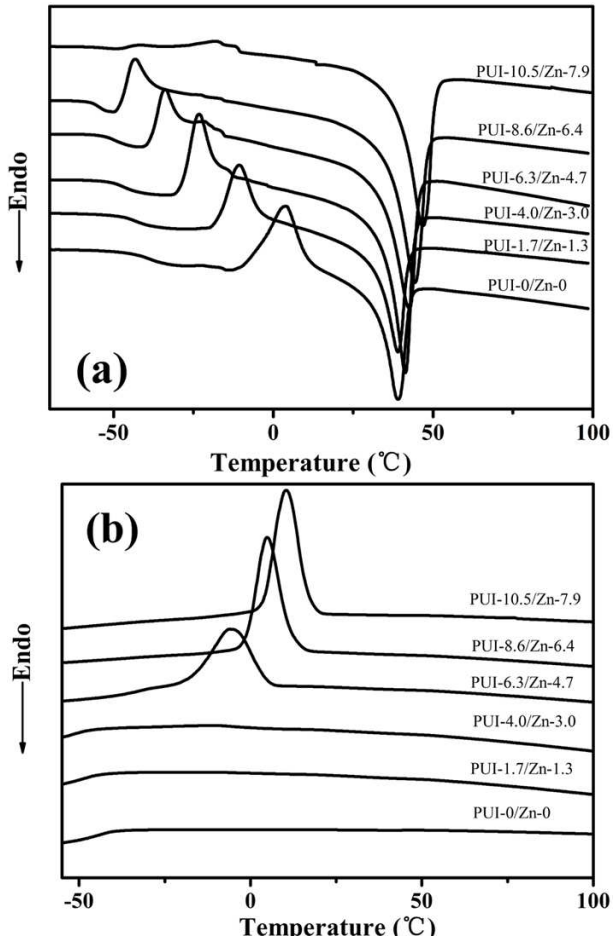

Fig. 4. DSC curves of PUI/$ZnCl_2$ complexes: (a) heating runs at rate of 10 °C min^{-1} after quick cooling with the liquid nitrogen, (b) subsequent cooling runs at 10 °C min^{-1}.

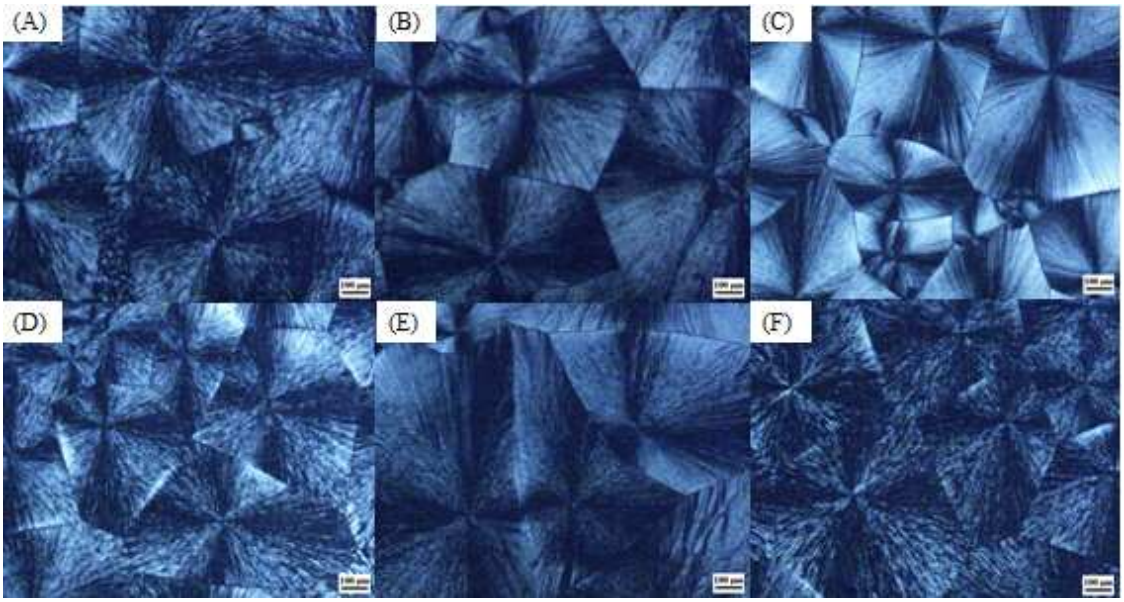

Fig. 5. Spherulitic morphologies formed after isothermally crystallized at 20 ℃ for PUI-0/Zn-0 (A), PUI-1.7/Zn-1.3 (B), PUI-4.0/Zn-3.0 (C), PUI-6.3/Zn-4.7 (D), PUI-8.6/Zn-6.4 (E) and PUI-10.5/Zn-7.9 (F).

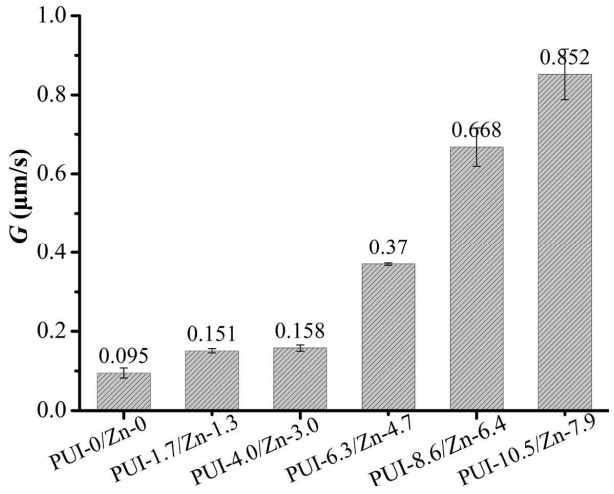

Fig. 6. The effect of ionic unit content on the spherulitic growth rate of PUI/$ZnCl_2$ complexes at 20 °C.

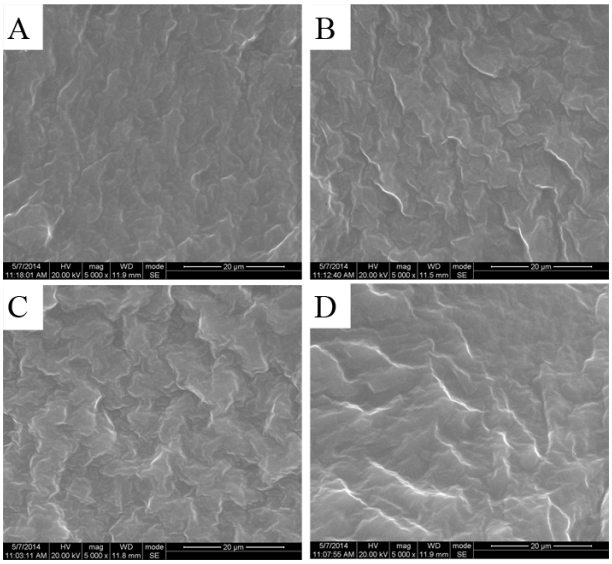

Fig. 7. SEM micrographs for cryo-fractured surfaces of PUI-0/Zn-0 (A), PUI-6.3/Zn-4.7 (B), PUI-8.6/Zn-6.4 (C), PUI-10.5/Zn-7.9 (D).

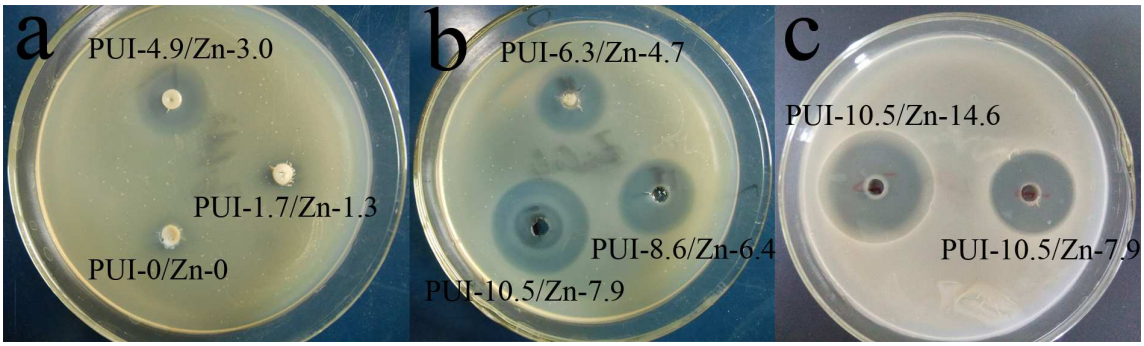

Fig. 8. The inhibition zones of complexes from PUI-0/Zn-0 to PUI-10.5/Zn-7.9 (a&b) at 48 h and of PUI-10.5/Zn-7.9 and PUI-10.5/Zn-14.6 (c) at 72 h against *E. coli*.

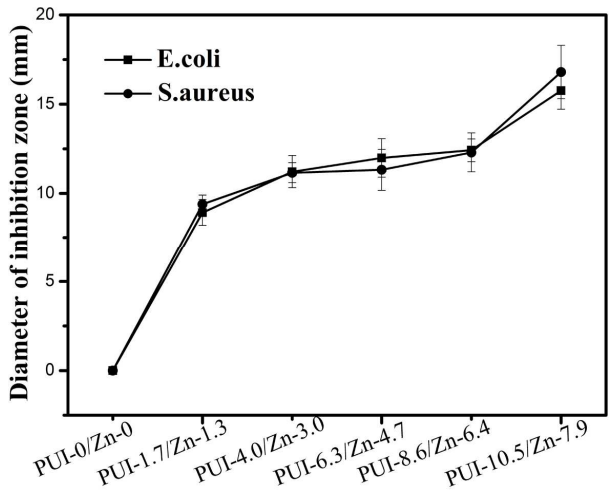

Fig. 9. Diameters of inhibition zones for evaluating antibacterial activity of PUI/$ZnCl_2$ complexes against *S. aureus* and *E. coli* at 48 h.

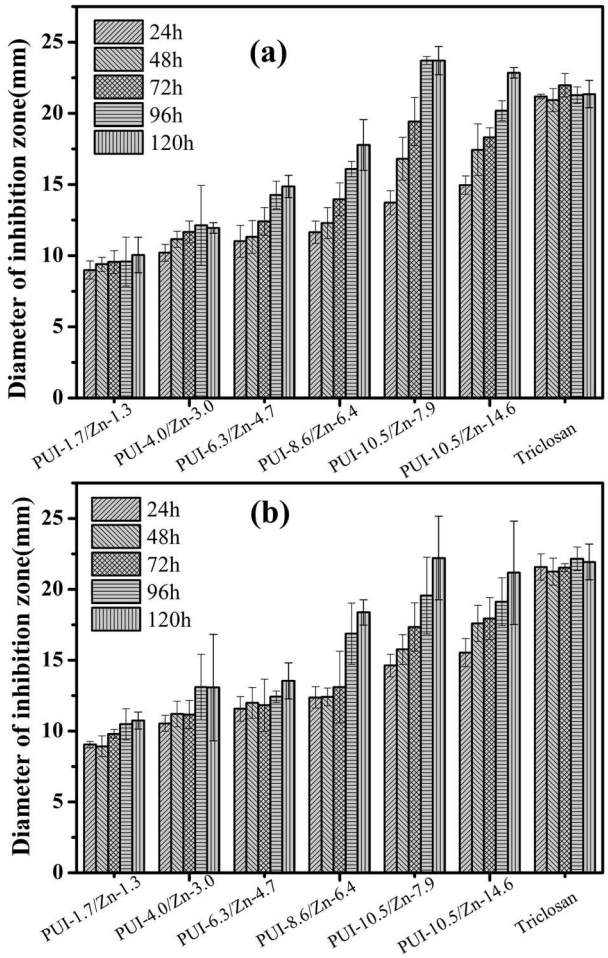

Fig. 10. Diameters of inhibition zones for evaluating the effect of time on the antibacterial activity of PUI/$ZnCl_2$ complexes and triclosan against *S. aureus* (a) and *E. coli* (b).

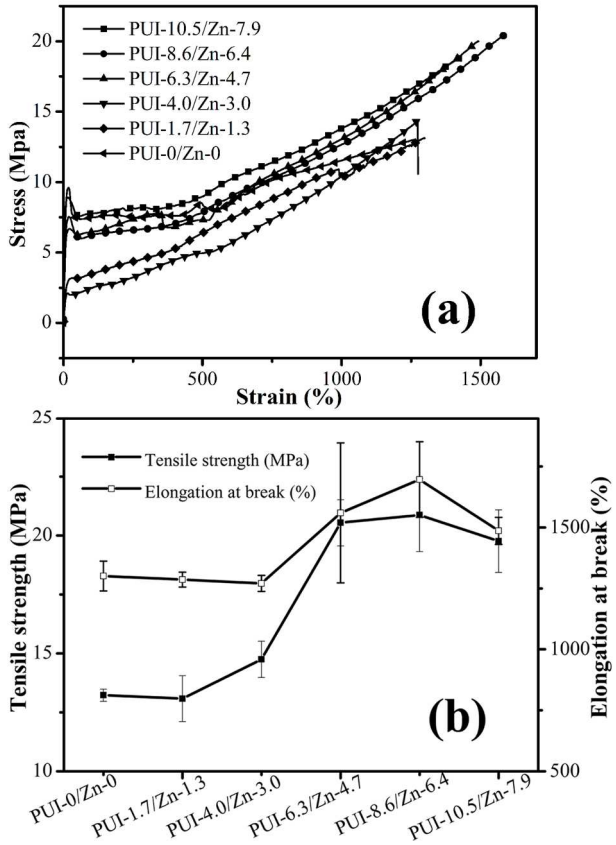

Fig. 11. (a) Stress-strain curves of PUI/$ZnCl_2$ complexes and (b) mechanical property parameters obtained from stress-strain measurement.